18

Optical and structural properties of semi-transparent flexible AgNWs/PET thin films

© D.M. Urazkulova[1], I.R. Boynazarov[1], A.Y. Turgunboev[1], Xin Li[2], Long Ye[2], Sunsun Li[3], E.A. Zakhidov[1], Sh.K. Nematov[4], V.O. Kuvondikov[1,¶]

[1] Institute of Ion-Plasma and Laser Technologies of the Uzbekistan Academy of Sciences, Tashkent, Uzbekistan
[2] School of Materials Science and Engineering, Joint Innovation Center of Chemical Science and Engineering of Tianjin University, Tianjin, China
[3] Flexible Electronics Laboratory of the Institute of Advanced Materials and School of Flexible Electronics of Nanjing University of Technology, Nanjing, China
[4] Shakhrisabz State Pedagogical Institute, Shakhrisabz, Uzbekistan

¶e-mail: vahobjon87@gmail.com

Received April 15, 2025
Revised May 09, 2025
Accepted May 20, 2025

In this work, silver nanowires (AgNWs) synthesized by the „Polyol" method were deposited on polyethylene terephthalate (PET) substrates in two layers using mechanical pressing, resulting in AgNWs/PET structures, and their physical properties were studied. It is shown that in this way it is possible to obtain AgNWs nanowires with a diameter of 50 ± 10 nm, a length of $15-20\,\mu$m and a density of $105-115$ mg/m^2 and a thin AgNWs/PET film with a resistance of 2.4 Ω/sq. The studied optical, electrical and structural characteristics of AgNWs/PET thin films confirm that they are a promising material as an electrode for flexible organic solar cells.

Keywords: AgNWs nanowires, PET substrate, transparent flexible electrode, absorption spectrum, transmission spectrum, Raman scattering.

DOI: 10.61011/EOS.2025.08.62027.7812-25

Introduction

At present, ensuring the population with affordable, safe, and environmentally friendly energy is one of the main tasks of the global community. Thin-film Organic Solar Elements (OSEs), as a promising type of next-generation photovoltaic technologies, can serve as an effective solution to this problem. Thanks to a number of key advantages, such as a low carbon footprint, the possibility of processing at low temperatures, simplicity of the production process, and most importantly, the possibility of manufacturing in the form of flexible structures, this type of OSE has recently been intensively studied to further enhance these competitive advantages for wide practical application [1–3].

In solar cells, the electrode material plays a key role in achieving high efficiency in converting light energy, since the degree of light entering the active layer and the efficiency of collecting photogenerated charges depend on the optical and photoelectric properties of the electrode material. The use of semi-transparent electrodes with fairly high light transmission over a wide spectral range and simultaneously low electrical resistance is a key solution to this problem [4–6].

To ensure high functionality of flexible OSEs, the semi-transparent electrodes used in them, along with high light transmittance and low surface electrical resistance, must also possess optimal surface functionality, mechanical flexibility, and thermal stability [7,8]. One of the widely used materials in photovoltaics and optoelectronics that meets most of these requirements is indium tin oxide, ITO. Among metal oxides, ITO demonstrates the most suitable physical properties for such requirements: its thin (100 nm) film deposited on a glass substrate has surface electrical resistance of around 20 Ω/sq, and light transmittance up to 90% [9]. However, the widespread use of this metal oxide brings several severe challenges owing to the high material cost, complexity of the manufacturing-technological process, the need to work under high vacuum and at high temperatures, as well as low transmittance in the infrared range [9]. A critical problem for the development of flexible OSEs is that thin ITO films on flexible substrates quickly crack under mechanical stresses. It should also be noted that in many cases in OSEs with thin ITO films on flexible substrates, the levels of light transmittance and electrical resistance often do not allow achieving optimal device parameters [4]. Based on this, modern flexible OSEs increasingly use carbon and metallic nanostructures as transparent electrodes. In particular, silver nanowires, AgNWs, possessing high electrical conductivity and sufficient transparency, are actively investigated as promising materials

for use in flexible OSEs [10,11]. For application in OSE development, AgNWs have several undeniable advantages: (i) high conductivity due to the low electrical resistance of silver; (ii) high light transmittance of AgNWs nanowire layers deposited on polymer films; (iii) the possibility of manufacturing flexible electrodes for flexible OSEs [12,13]. Furthermore, it should be noted that the AgNWs synthesis method is quite simple, and their corresponding structures can be processed using solutions, including with the use of the most environmentally friendly solvent — water [14]. Therefore, AgNWs are considered the most accessible and alternative solution to ITO for creating next-generation flexible OSEs. To achieve the necessary quality, structural properties, and long-term stability of such nanowires, active research is currently underway, in particular to identify the nature of agglomeration in the AgNWs structure, which causes the nanowires to adhere to each other, significantly reducing their electrical conductivity [15].

An important property of AgNWs, which opens new opportunities for application in OSE development, is the ability of networks of such nanowires to scatter light. Intense light scattering and a high level of haze — a physical parameter characterizing this phenomenon, as shown in studies [16], — lead to a significant increase in solar cell efficiency; for this, the content of AgNWs on the polyethylene terephthalate (PET) substrate must exceed 10 mg/m^2. In this case, haze determines the degree of light passing into the light-absorbing active layer. In addition, it has been established that increasing the level of haze of the AgNWs nanowires not only lengthens the light propagation path but also contributes to improving the short-circuit current density in OSEs [17]. Increasing the haze level in thin AgNWs films causes significant light scattering, lengthening the optical path, thereby providing longer retention of light inside the active layer. Such elongation of the light path plays a key role in increasing light absorption, which contributes to improving conversion efficiency.

Thus, conducted studies indicate that the efficiency of OSEs depends both on the sizes of AgNWs nanowires and their optical parameters such as light transmittance and absorption, as well as the level of haze. Taking this into account, in the present work, the optical and structural characteristics of AgNWs/PET have been studied to identify the possibilities of using such structures as transparent electrodes for flexible OSEs.

Materials and Methods

Synthesis of AgNWs/PET films. Silver nanowires (AgNWs) were synthesized by the „polyol“ method and deposited on polyethylene terephthalate (PET) substrates using two-stage mechanical pressing. The following reagents were used to synthesize AgNW nanowires: silver nitrate ($AgNO_3$, $\geq$ 99%, Sigma-Aldrich, USA), polyvinylpyrrolidone (PVP, Sigma-Aldrich, USA), sodium chloride (NaCl), and ethanol (Sigma-Aldrich, USA). A membrane made of polyvinylidene fluoride (PVDF) was used in the process of obtaining AgNW nanowires. Preparation of the silver nanowire solution was carried out as follows. 100 ml of PVP was dissolved in ethanol at a concentration of 0.1 mol/l and heated in a flask to 150 °C for 1 hour under continuous magnetic stirring. Then, 100 μl of NaCl solution in ethanol with a concentration of 0.1 mol/l was added to the flask. After 5 minutes, 150 ml of $AgNO_3$ solution in ethanol at 0.1 mol/l concentration was introduced into the flask at a rate of 10 ml/min. A suspension of AgNWs dissolved in ethanol at a concentration of 5 mg/ml was prepared. The resulting solution was cooled to room temperature, filtered through a membrane filter with pore size 0.8 μm and diluted with deionized water. Then, the AgNWs collected on the membrane filter were redispersed in deionized water using ultrasound. As a result, a silver nanowire solution with a concentration of 4 μg/ml in deionized water was obtained. The resulting solution was filtered for 30 minutes through a polyvinylidene fluoride (PVDF) membrane, after which this process was repeated to create two identical AgNWs/PVDF samples. In the next step, the PVDF membrane with the AgNWs coating was transferred onto a PET substrate using mechanical pressing at a pressure of 2 MPa for 10 seconds, after which the filtering membrane was carefully removed. After this, the samples with AgNWs/PET were air-dried for 10 minutes, and then a second layer of AgNWs/PVDF was applied from above in the same manner. The main goal of double deposition of AgNWs on the PET substrate was to ensure high electrical conductivity and low resistance despite some reduction in light transmittance. To increase the density of nanowires in the AgNWs/PET film and the corresponding improvement of electrical conductivity, repeated mechanical pressing was carried out at a pressure of 15 MPa for 25 seconds.

Similar methods of synthesis and structure formation of AgNWs/PET were applied in other studies [18,19]. However, unlike them, we used a two-layer coating to obtain an AgNWs/PET structure with reduced electrical resistance (Fig. 1).

Characterization of AgNWs/PET films. Absorption and transmission spectra of thin AgNWs/PET films in the range of 190–1100 nm were measured using a Cary 60 spectrophotometer (Agilent, USA). Photoluminescence (PL) spectra of thin-film AgNWs/PET samples in the range of 400–800 nm were measured with an RF 6000 spectrofluorimeter (Shimadzu, Japan) under excitation by monochromatic light with a wavelength of 380 nm. Scanning electron microscopy (SEM) images of AgNWs on PET substrates were obtained using a Zeiss EVO MA 15 microscope (Carl Zeiss, Germany) at an accelerating voltage of 5.00 kV, and transmission electron microscopy (TEM) images were taken with an H-7650 microscope (Hitachi, Japan) at a scale of 500 nm. Raman scattering spectra were measured with an InVia Raman 2000 spectrometer (Renishaw, UK) under 10 mW excitation power at 532 nm wavelength using a 50x microobjective. X-ray diffraction (XRD) was studied with

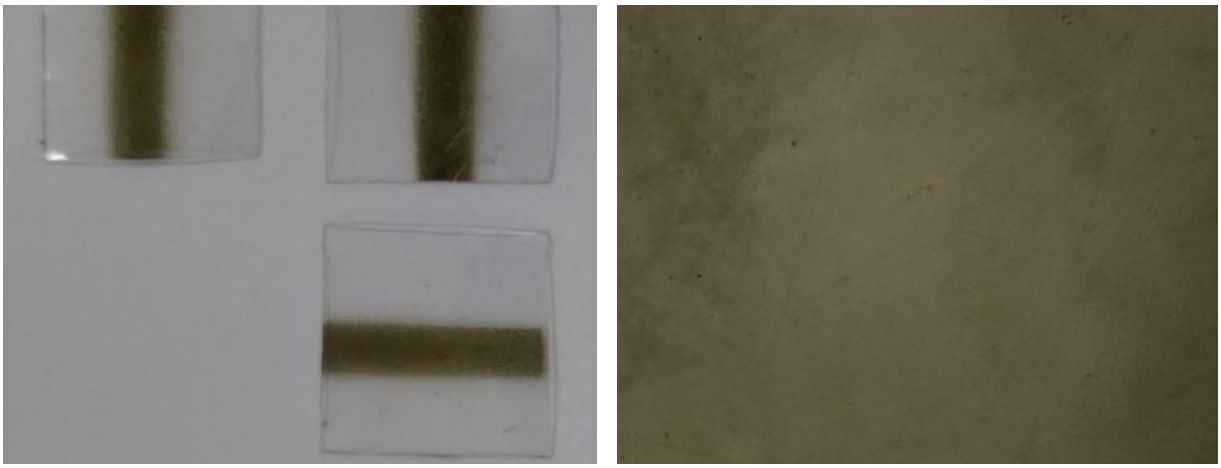

Figure 1. General view of AgNWs samples deposited on PET substrates.

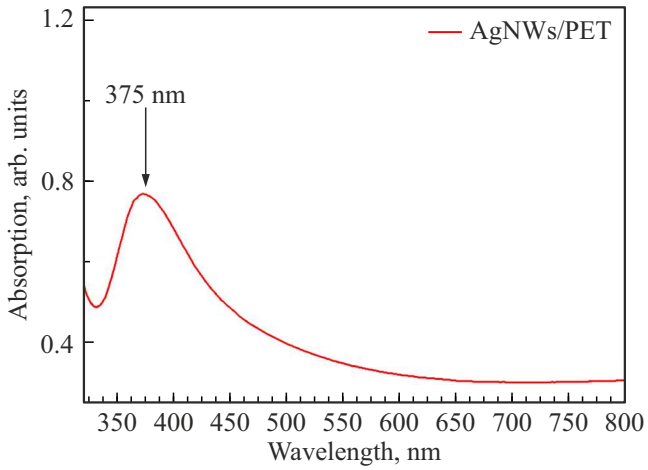

Figure 2. Absorption spectrum of the AgNWs/PET structure.

an XRD-6100 diffractometer (Shimadzu, Japan) at Bragg angles 2θ from 5 to 80°. The surface resistance of the thin AgNW film was measured by the four-point probe method using a Four-Point Probe Plus device (Osilla, UK).

Results and Discussion

As is known, the absorption spectra of the AgNWs/PET structure depend on the nanowires' sizes, their structural features, as well as the method and conditions of synthesis. The spectrum shows clearly defined maxima related to localized plasmon resonance (LPR). The transverse LPR mode in AgNWs depends on their diameter and surface morphology and typically appears in the absorption spectrum as an intense band in the 380–400 nm region [20]. This band can shift toward the „red" or „blue" regions of the spectrum depending on the nanowire diameter. For example, for nanowires with a diameter of 40–60 nm the absorption peak is observed at 380 nm, while for a diameter of 70–100 nm the absorption band shifts closer to 400 nm [21,22]. The longitudinal LPR mode in AgNWs depends on their length and ordering, with the corresponding absorption band expected to lie in the near-infrared region [21]. In the absorption spectrum of the studied AgNWs/PET samples, a relatively broad absorption band was observed in the 350–415 nm region with a maximum at 375 nm (Fig. 2). This indicates that the diameter of the examined AgNWs lies within 40–70 nm, with most nanowires having a diameter around 50 nm. In most cases, the absorption band of AgNWs synthesized by the „polyol" method and related to LPR was observed in the 370–410 nm region [23]. Note that the AgNWs samples studied in this work may differ significantly in structure and characteristic sizes from samples obtained by other researchers, as the physical synthesis conditions could vary considerably.

The density and diameter of the nanowires, as well as the synthesis methods of AgNWs, significantly influence their transmission spectra. It is known that increasing the nanowire density improves electrical conductivity but decreases optical transparency. Therefore, finding an optimal balance between optical transmittance and electrical conductivity plays a decisive role in the application of such flexible electrodes. Xiang-Qian and his team synthesized AgNWs with optimal parameters by the „Transfer-printing and secondary pressing" method: at a minimum electrical resistance 11.5 Ω/sq the light transmittance at 550 nm (T□□□) was 93.4% [18]. Wei Xu and his group found that for AgNWs synthesized by the „polyol" method and deposited on PET substrates with a density of 16 mg/m^2, the light transmittanceT_{550} was 82.3%, while increasing the density to 80 mg/m^2 T_{550} reduced to 65.6% [24].

Figure 3 shows the transmission spectra of the PET polymer film and the AgNWs/PET structure of the samples we studied. As seen from the spectra, at a wavelength of 715 nm the transmittance reaches a maximum value of 50%, while at 550 nm it is 45%. From these data, it can be

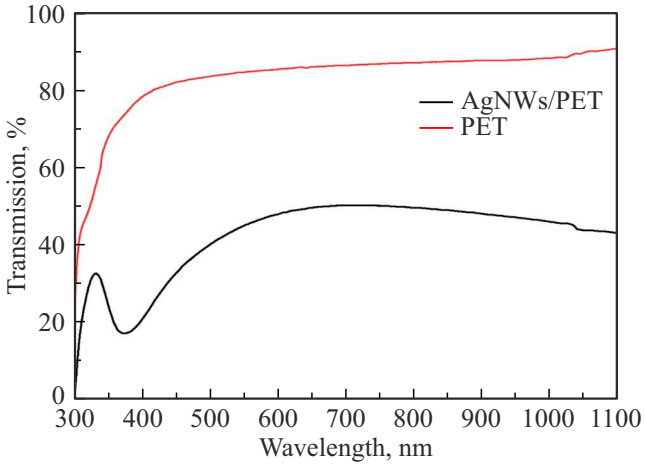

Figure 3. Transmission spectrum of the PET polymer film and the AgNWs/PET structure.

estimated that the AgNWs density in the studied samples was quite high — about 105–115 mg/m^2. Compared with the results presented in work [24], the AgNWs/PET density in our samples is 7 times higher, which decreases optical transparency but significantly increases electrical conductivity.

The transmission spectrum of the AgNWs/PET samples is also strongly influenced by the light transmittance of the PET substrate itself. The $T_{550} = 84.6\%$ value in PET indicates that its transmission spectrum is not ideal. The transmittance coefficient of the AgNWs layer without the substrate can be calculated by the formula:

$$T_f = \frac{T_{f+s}}{T_s}, \qquad (1)$$

where T_f is the light transmittance coefficient of the AgNWs layer, T_s is the light transmittance coefficient of the PET substrate, T_{f+s} is the transmittance coefficient of the AgNWs/PET structure [25]. The resulting value of $T_{550} = 53\%$ indicates a high density of Ag nanowires capable of providing minimal resistance.

A key advantage of our AgNWs/PET samples is maintaining light transmittance above 43% in the infrared region, up to 1100 nm, while also achieving a minimum electrical resistance of 2.4 Ω/sq. These parameters demonstrate that organic solar elements based on such electrodes can simultaneously realize efficient charge transport with minimal losses and utilize light over a wide spectral range. The transmission spectrum shows a sharp drop around 375 nm, which corresponds to an absorption band related to LPR caused by AgNWs. The PL spectra of AgNWs nanowires depend on LPR properties, morphology, and the nature of their interaction with the substrate [26]. In most cases, depending on the size characteristics of AgNWs, PL bands appear in the 350–600 nm range, consisting of various plasmon resonance modes [26–28]. Other researchers also observed PL bands in the corresponding spectral range for nanowires with a diameter of 50–70 nm and explained this by electron localization on the surface [29]. When the density of AgNWs is high, corresponding plasmonic responses in their PL spectra manifest with high intensity.

We also studied the PL spectra of AgNWs samples under excitation with a wavelength of 380 nm, in the region corresponding to nanowire absorption (Fig. 4). The PL spectrum showed a broad band in the 400–650 nm region with a maximum at 460 nm, associated with transverse plasmon resonances. The width of this band and its asymmetric shape with an extended right shoulder indicate the presence of a significant number of nanowires with large diameters in the structure [30]. However, it should be noted that the PL spectra of AgNWs may vary slightly depending also on synthesis conditions, surface state, oxidation, and type of polymer substrate [27,29].

To clarify the dominant photoluminescence mechanism, we decomposed the measured PL spectra of our AgNWs samples, which present an asymmetrical broad band, into Gaussian components. This helps to identify the electronic transitions responsible for PL, the influence of defects, and plasmonic effects, ultimately establishing the corresponding optical, electronic, and morphological characteristics of AgNWs. Four Gaussian components were distinguished in the experimentally measured PL spectrum of the studied AgNWs samples (Fig. 4) with maxima at 435, 460, 500, and 540 nm, which can be interpreted as follows:

1. Component (band) *1* with a maximum at 435 nm (2.85 eV) may be associated with transverse (perpendicular to the nanowire axis) surface plasmon resonances of AgNWs. The corresponding electronic transition may be linked to structural defects of the nanowires [31].

2. Component (band) *2* with a maximum at 460 nm (2.7 eV) may be related to surface defects and charge carrier recombination in AgNWs with an average diameter of ∼ 50 nm [32,33].

3. Component (band) *3* with a maximum at 500 nm (2.48 eV) may be associated with the longitudinal (along

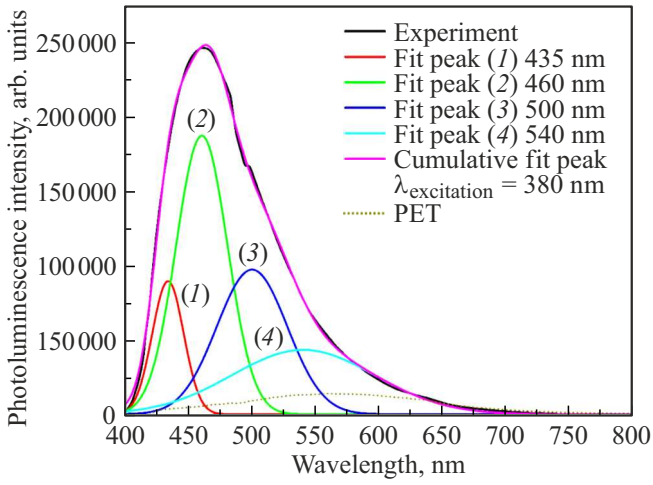

Figure 4. PL spectrum of AgNWs/PET film and four Gaussian components into which it is decomposed.

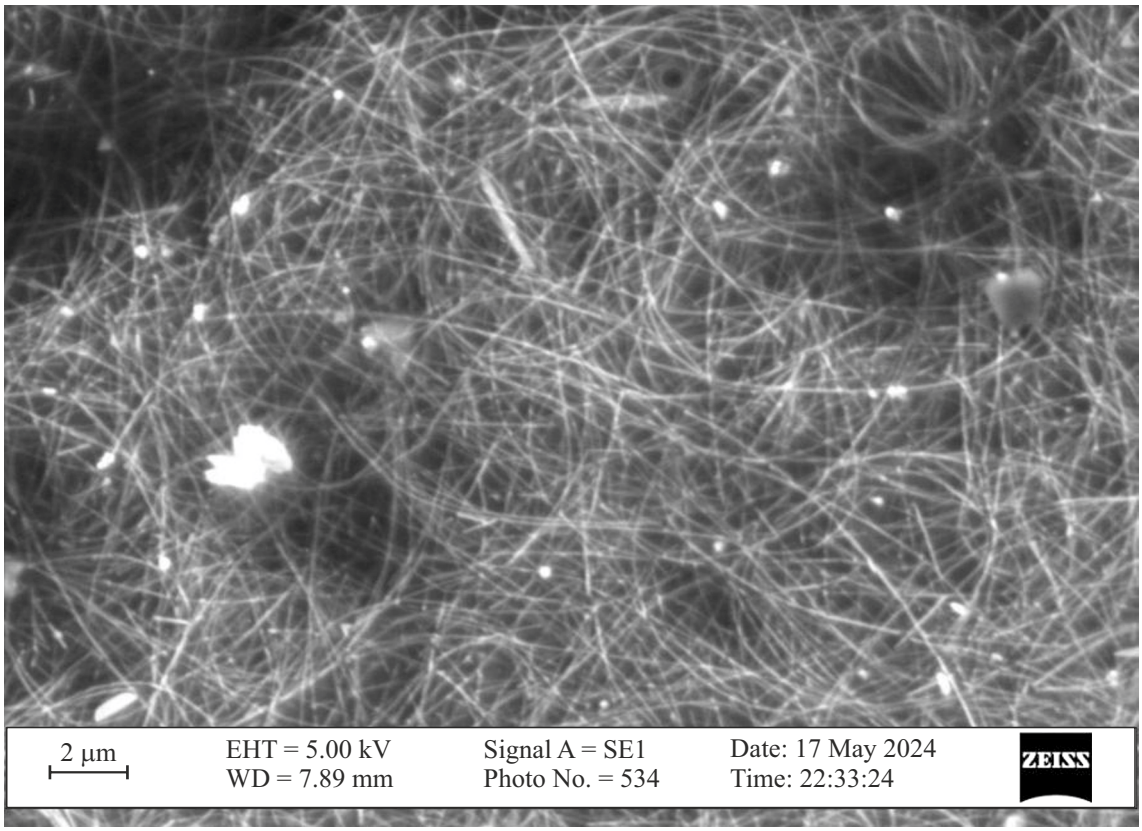

Figure 5. SEM image of the AgNWs/PET structure.

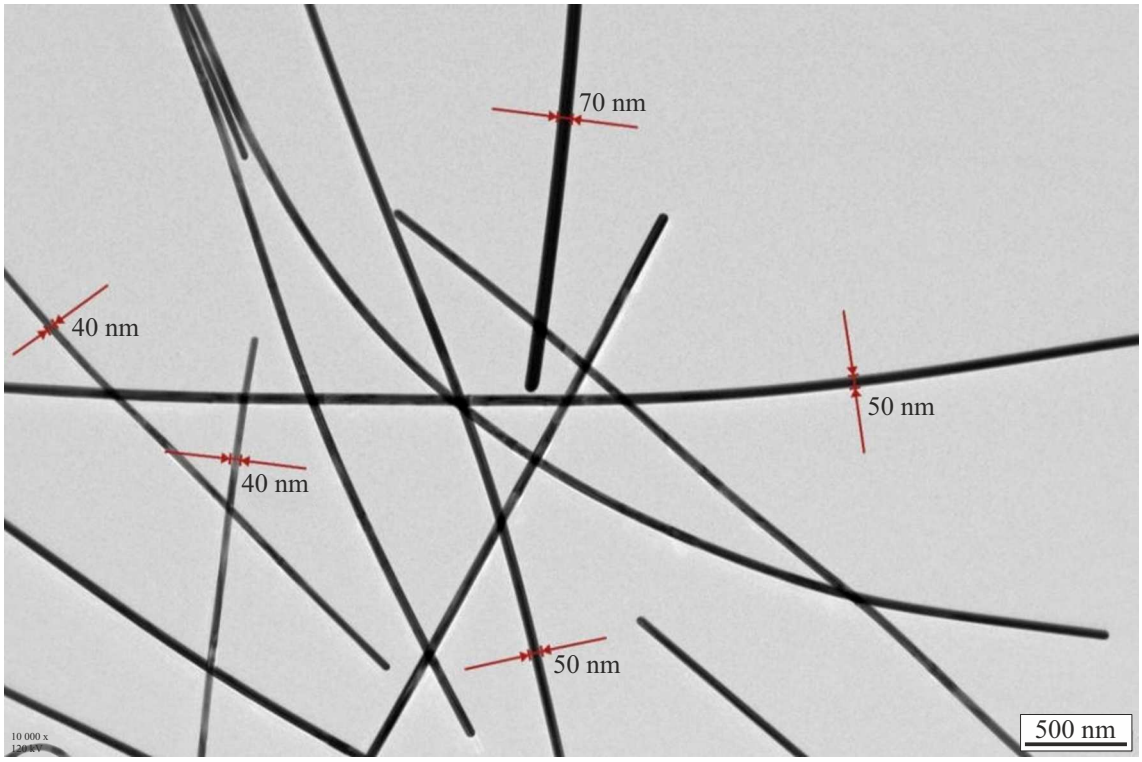

Figure 6. TEM image of the AgNWs/PET structure.

the nanowire axis) surface plasmon resonance, indicating the presence of longer nanowires. This resonance depends on the aspect ratio of nanowire length to diameter [30,34].

4. Component (band) *4* with a maximum at 55 nm (2.3 eV) may be linked to longitudinal surface plasmon resonance in AgNWs with a large diameter ($\sim$ 100 nm) and length $\sim 50\,\mu$m [30,35].

Transverse surface plasmon resonance bands at shorter wavelengths in the PL spectrum indicate the presence of nanowires with smaller diameters. The high intensity of band *2* with a maximum at 460 nm in Fig. 4 indicates a large percentage of nanowires with a diameter of about 50 nm in the studied AgNWs samples. We also measured the photoluminescence spectrum of a pure PET film without Ag nanowires (Fig. 4). The photoluminescence intensity of the thin PET film was very low compared to the AgNW/PET sample. It is evident that the photoluminescence of pure PET practically does not affect the overall photoluminescence spectrum of the AgNW/PET structure.

To study morphology, diameter and length distribution, and the ordering of AgNWs nanowires, the most informative method is scanning electron microscopy (SEM) [14,20]. The SEM image of the examined AgNWs/PET samples showed that in such a structure silver nanowires are arranged chaotically, interweaving into a dense structure resembling hair fibers (Fig. 5). From the figure one can estimate the average nanowire length, which turned out to be quite large, $15-20\,\mu$m. This confirms that the AgNWs/PET structure, possessing a high degree of flexibility, can be a suitable material as an electrode for flexible organic solar elements (OSEs). White dots and clusters are also observed in the SEM images, possibly formed as a result of agglomeration, oxidation, or uncontrolled synthesis residues. The nanowire arrangement is generally uniform, with some regions where nanowires intertwine and form clusters.

SEM images also indicate that AgNWs have high uniformity and sufficient density, indicating their high quality for use as flexible electrodes in various flexible electronics applications.

TEM microscopy imaging allows more precise determination of layer morphology, diameter, length, and aspect ratio (length/diameter) of AgNWs [36]. Depending on the synthesis method, silver nanowire diameters typically vary from 20 to 150 nm, and lengths range from 5 up to 50 μm. For example, in several works using the „polyol“ method, AgNWs with diameters of 20 nm and lengths of 40 μm were obtained, corresponding to an aspect ratio of 2000 [37].

Analysis of TEM images of the studied AgNWs samples showed that the average nanowire diameter is 50 nm, although individual occurrences of diameters 40 nm and 70 nm were also observed (Fig. 6). The figure shows that despite the straight nanowire shape on the nanoscale, at the microscale, the nanowires exhibit strong curvature and reach several microns in length. Additionally, the nanowire diameters do not vary significantly from one another, indicating their high uniformity. A large aspect ratio of such nanowires also confirms their promise for use as flexible electrodes in relevant applications.

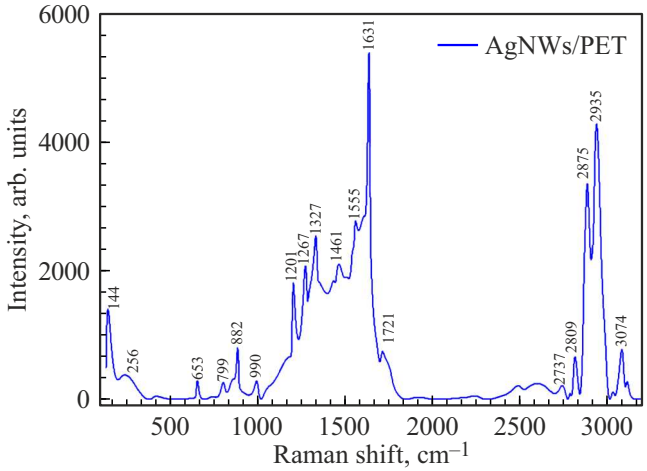

Figure 7. Raman scattering spectra of the AgNWs/PET structure.

Raman scattering spectroscopy is an important tool for studying the structural characteristics of AgNWs nanowires [38,39]. Considering this, we measured the Raman scattering spectra of AgNWs/PET samples (Fig. 7). In the Raman spectrum of the AgNWs/PET structure, key vibrational frequencies of silver nanowires were identified; they are listed in the table. Note that because it is not possible to focus all the laser radiation exclusively on the AgNWs layer which is less than 1 μm thick, the PET substrate several millimeters thick was also illuminated, so the spectrum also contains intense bands corresponding to PET vibrations. Usually, to achieve high light transmittance, the nanowire density of AgNWs is kept low. To maintain such conditions, i.e., control nanowire density, the Raman scattering peak at 256^{-1} cm associated with AgNWs vibrations in Fig. 7, can be used as an indicator [40]. The Raman spectrum also exhibits a band at 1721 cm^{-1} associated with ester and C=O vibrations, which allows evaluation of potential interactions between AgNWs and PET [25]. Thus, these characteristic peaks in the Raman spectrum can serve as informative indicators of nanowire density and their interaction with the film onto which they are deposited.

Structural characteristics and crystallinity degree of AgNWs can be determined using X-ray diffraction (XRD) [23]. Typically, the XRD spectra of AgNWs clearly display characteristic silver diffraction peaks (111) and (200) [25]. These peaks reflect crystal arrangement, deformation, and thermal stability. The XRD pattern of the AgNWs/PET structure was obtained over Bragg angles 2θ from 10 to 80° (Fig. 8). Analysis of this pattern gives the following interpretation for Bragg angles 2θ: (i) a broad band in the 10–30° range indicates the amorphous structure of the PET substrate; (ii) high-intensity peaks at 37.6, 43.8, 64.2 and 77.3° correspond to the crystalline nature of AgNWs [42]; and (iii) other low-intensity peaks may indicate phase interaction between AgNWs and PET substrate,

Characteristic vibrational frequencies identified in the Raman scattering spectrum of the AgNWs/PET structure

№	Frequency shift (cm^{-1})	Type of molecular vibration	Origin of vibration) (AgNWs or PET)
1	256	Ag-symmetric vibrations	Associated with low-frequency surface plasmon vibrations of AgNWs [40]
2	653	Vibrations related to with C−C- and C−O-bonds	One of the characteristic PET vibrational bands PET [25]
3	799	C−H-vibrations	
4	882	C−C-vibrations	
5	990	C−H-vibrations	
6	1201	C−O−C-deformation vibrations	Associated with molecular skeleton PET [25,41]
7	1267	C−H-vibrations	
8	1327	C−C-symmetric vibrations	
9	1461	C−H-vibrations	Related to PET-characteristic benzene ring vibrations [25]
10	1555	Aromatic C=C vibrations	
11	1631	C=O carbonyl vibrations	
12	1721	Ester C=O vibrations	Vibrations typical for PET [25]
13	2737, 2809, 2875, 2935, 3074	C−H-Symmetric and asymmetric vibrations	Vibrations belong to methylene and methyl groups of PET [25,41]

as well as oxidation, contamination, or presence of small amounts of other phases. AgNWs generally have a face-centered cubic (FCC) structure, and strong diffraction peaks correspond to Ag (111), Ag (200), Ag (220), Ag (311). In this case, the Bragg angles 2θ correspond to the following orientations: (111) — 37.6°, (200) — 43.8°, (220) — 64.2°, (311) — 77.3° [25,42]. The sizes, density, and synthesis conditions of silver nanowires can also cause shifts in Bragg angles 2θ or changes in average peak widths [43]. Moreover, the peak observed at 56.2° in the diffraction pattern relates to silver oxide (Ag−O), which can form due to partial oxidation of AgNWs [25,37]. Although the PET polymer substrate usually has an amorphous structure, in some cases it can display some crystallinity due to ordered polymer chains. In our samples, peaks observed at Bragg angles 2θ at 16.4° and 22.6° suggest the possible presence of crystalline PET phases formed by ordered polymer chains [43].

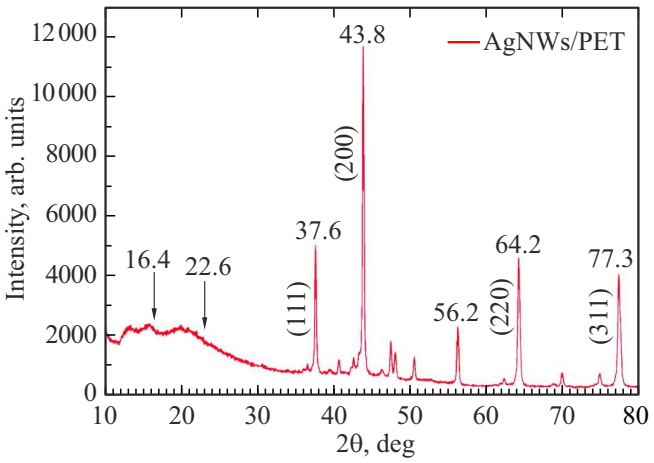

Figure 8. X-ray diffraction pattern of the AgNWs/PET structure.

Conclusion

This work studied AgNWs synthesized by the „polyol" method and deposited on PET substrates by mechanical pressing, forming a two-layer AgNWs/PET structure with resistance 2.4 Ω/sqand nanowire density 105−115 mg/m^2. Despite low light transmission in the visible range ($T_{550} = 45\%$), the obtained AgNWs/PET samples demonstrated rather high light transmittance in the IR range ($T_{550} = 43\%$) at wavelengths up to 1100 nm. Analysis of the PL spectrum of the AgNWs/PET structure with Gaussian decomposition showed that the intense band with a maximum at 460 nm, associated with transverse surface plasmon resonance, indicates the predominance of nanowires with small diameters in this structure. Using SEM, TEM imaging and optical spectra analysis of synthesized AgNWs samples, important data on nanowire sizes and morphology were obtained. According to these data, most nanowires have a diameter of about 50 nm and lengths reach 15−20 μm. The aspect ratio (length/diameter) of such nanowires at the level of 300−400 characteristic morphology, and random but dense packing of AgNWs provide broad prospects for using such structures as flexible electrodes in new flexible OSEs with active layers adaptable to a wide light spectrum.

Acknowledgments

The author would like to thank Doctors Xin Li and Long Ye, scientists from the School of Materials Science and Engineering of Tianjin University, for their close cooperation and assistance in obtaining TEM images of the AgNW/PET structure.

Funding

This work was performed with the support of project AL-8724053065, provided by the Agency for Innovative Development of the Republic of Uzbekistan.

Conflict of interest

The authors declare that they have no conflict of interest.

References

[1] X. Sun, F. Wang, G. Yang, X. Ding, J. Lv, Y. Sun, T. Wang, C. Gao, G. Zhang, W. Liu, X. Xu, S. Satapathi, X. Ouyang, A. Ng, L. Ye, M. Yuan, H. Zhang, H. Hu. Energy Environ. Sci., **18**, 2536 (2025). DOI: 10.1039/D4EE05533K

[2] D. Qiu, C. Tian, H. Zhang, J. Zhang, Z. Wei, K. Lu. Adv. Mater., **36**, 2313251 (2024). DOI: 10.1002/adma.202313251

[3] J. Lv, X. Sun, H. Tang, F. Wang, G. Zhang, L. Zhu, J. Huang, Q. Yang, S. Lu, G. Li, F. Laquai, H. Hu. InfoMat **6**, e12530 (2024). DOI: 10.1002/inf2.12530

[4] M.R. Azani, A. Hassanpour, T. Torres. Adv. Energy Mater., **10**, 2002536 (2020). DOI: 10.1002/aenm.202002536

[5] Y. Fang, Z. Wu, J. Li, F. Jiang, K. Zhang, Y. Zhang, Y. Zhou, J. Zhou, B. Hu. Adv. Funct. Mater., **28**, 1705409 (2018). DOI: 10.1002/adfm.201705409

[6] E. Zakhidov, A. Kokhkharov, V. Kuvondikov, S. Nematov, R. Nusretov. J. Korean Phys. Soc., **67**, 1262 (2015). DOI: 10.3938/jkps.67.1262

[7] Y. Bae, D. Kim, S. Li, Y. Choi, S.Y. Son, T. Park, L. Ye. Prog. Polym. Sci., **159**, 101899 (2024). DOI: 10.1016/j.progpolymsci.2024.101899

[8] S. Zeng, H. Li, S. Liu, T. Xue, K. Zhang, L. Hu, Z. Cai, Y. Cui, H. Wang, M. Zhang, X. Hu, L. Ye, Y. Song, Y. Chen. Energy Environ. Sci., **18**, 2318 (2025). DOI: 10.1039/D4EE02963A

[9] S. De, J.N. Coleman. MRS Bull., **36**, 774 (2011). DOI: 10.1557/mrs.2011.236

[10] K. Yang, Z. Wang, J. Zhang. Opt. Laser Technol., **164**, 109533 (2023). DOI: 10.1016/j.optlastec.2023.109533

[11] S. Nam, M. Song, D.H. Kim, B. Cho, H.M. Lee, J.D. Kwon, S.G. Park, K.S. Nam, Y. Jeong, S.H. Kwon, Y.C. Park, S.H. Jin, J.W. Kang, S. Jo, C.S. Kim. Sci. Reports., **4**, 1 (2014). DOI: 10.1038/srep04788

[12] W. Li, H. Zhang, S. Shi, J. Xu, X. Qin, Q. He, K. Yang, W. Dai, G. Liu, Q. Zhou, H. Yu, S.R.P. Silva, M. Fahlman. J. Mater. Chem. C., **8**, 4636 (2020). DOI: 10.1039/C9TC06865A

[13] F. Basarir, F.S. Irani, A. Kosemen, B.T. Camic, F. Oytun, B. Tunaboylu, H.J. Shin, K.Y. Nam, H. Choi. Mater. Today Chem., **3**, 60 (2017). DOI: 10.1016/j.mtchem.2017.02.001

[14] L. Zhang, T. Song, L. Shi, N. Wen, Z. Wu, C. Sun, D. Jiang, Z. Guo. J. Nanostructure Chem., 2021 113 **11**, 323 (2021). DOI: 10.1007/s40097-021-00436-3

[15] X. Yu, X. Yu, L. Chen, J. Zhang, Y. Long, L. Zhe, J. Hu, H. Zhang, Y. Wang. Opt. Mater., **84**, 490 (2018). DOI: 10.1016/j.optmat.2018.07.048

[16] B.Y. Wang, T.H. Yoo, J.W. Lim, B.I. Sang, D.S. Lim, W.K. Choi, D.K. Hwang, Y.J. Oh. Small., **11**, 1905 (2015). DOI: 10.1002/smll.201402161

[17] C. Preston, Y. Xu, X. Han, J.N. Munday, L. Hu. Nano Res., **6**, 461 (2013). DOI: 10.1007/s12274-013-0323-9

[18] M. xiang Jing, M. Li, C. yu Chen, Z. Wang, X. qian Shen. J. Mater. Sci., **50**, 6437 (2015). DOI: 10.1007/s10853-015-9198-3

[19] M. Li, M. Jing, Z. Wang, B. Li, X. Shen. J. Nanosci. Nanotechnol., **15**, 6088 (2015). DOI: 10.1166/jnn.2015.10283

[20] M. Oh, W.Y. Jin, H. Jun Jeong, M.S. Jeong, J.W. Kang, H. Kim. Sci. Reports., **5**, 1 (2015). DOI: 10.1038/srep13483

[21] B. Park, I.G. Bae, Y.H. Huh. Sci. Reports., **6**, 1 (2016). DOI: 10.1038/srep19485

[22] S. Fahad, H. Yu, L. Wang, Y. Wang, T. Lin, B.U. Amin, K.U.R. Naveed, R.U. Khan, S. Mehmood, F. Haq, Y. Xing, M. Usman. J. Electron. Mater., **50**, 2789 (2021). DOI: 10.1007/s11664-021-08770-6

[23] B.A. Kale, S.N. Birajdar, P.U. More, P.V. Adhyapak. J. Mater. Sci. Mater. Electron., **35**, 1 (2024). DOI: 10.1007/s10854-024-12087-5

[24] W. Xu, Q. Xu, Q. Huang, R. Tan, W. Shen. W. Song, J. Mater. Sci. Technol., **32**, 158 (2016). DOI: 10.1016/j.jmst.2015.12.009

[25] A. Voronin, I. Bril., A. Pavlikov, M. Makeev, P. Mikhalev, B. Parshin, Y. Fadeev, M. Khodzitsky, M. Simunin, S. Khartov. Polymers (Basel)., **17**, 321 (2025). DOI: 10.3390/polym17030321

[26] S. Dong, W. Zhang, M. Qi, A. Wei, G. Zhang, R. Chen, J. Hu, M. Bai, Z. Yang, X. Liu, L. Xiao, C. Qin, S. Jia. ACS Photonics., **12**, 1 (2025). DOI: 10.1021/acsphotonics.4c01886

[27] V. Kravets, Z. Almemar, K. Jiang, K. Culhane, R. Machado, G. Hagen, A. Kotko, I. Dmytruk, K. Spendier, A. Pinchuk. Nanoscale Res. Lett., **11**, 1 (2016). DOI: 10.1186/s11671-016-1243-x

[28] M. Hamzah, M. Khenfouch, V.V. Srinivasu. J. Mater. Sci. Mater. Electron., **28**, 1804 (2017). DOI: 10.1007/s10854-016-5729-1

[29] J. Jiu, T. Sugahara, M. Nogi, K. Suganuma. J. Nanoparticle Res., **15**, 1 (2013). DOI: 10.1007/s11051-013-1588-3

[30] J.J. Mock, M. Barbic, D.R. Smith, D.A. Schultz, S. Schultz. J. Chem. Phys., **116**, 6755 (2002). DOI: 10.1063/1.1462610

[31] J. Niedziółka-Jönsson, S. Mackowski. Mater., **12**, 1418 (2019). DOI: 10.3390/ma12091418

[32] S. Link, M.A. El-Sayed. J. Phys. Chem. B., **103**, 8410 (1999). DOI: 10.1021/jp9917648

[33] D.D. Evanoff, G. Chumanov. J. Phys. Chem. B., **108**, 13957 (2004). DOI: 10.1021/jp0475640

[34] P.K. Jain, M.A. El-Sayed. Chem. Phys. Lett., **487**, 153 (2010). DOI: 10.1016/j.cplett.2010.01.062

[35] V.O.Bolshakov, K.V. Prigoda, A.A. Ermina, D.P. Markov, Yu.A. Zharova. Opt. Spectrosc., **132 : 12**, 1240–1243, (2024). DOI: 10.61011/OS.2024.12.59801.6451-24

[36] Y.-H. Hsueh, A. Ranjan, L.-M. Lyu, K.-Y. Hsiao, Y.-C. Chang, M.-P. Lu, M.-Y. Lu, M.-Y. Lu. Adv. Electron. Mater., **9**, 2201054 (2023). DOI: 10.1002/aelm.202201054

[37] M.B. Gebeyehu, T.F. Chala, S.Y. Chang, C.M. Wu, J. Y. Lee. RSC Adv., **7**, 16139 (2017). DOI: 10.1039/C7RA00238F

[38] X. Zhu, A. Guo, Z. Yan, F. Qin, J. Xu, Y. Ji, C. Kan. Nanoscale., **13**, 8067 (2021). DOI: 10.1039/D1NR00977J
[39] E.A. Zakhidov, M. A. Zakhidova, A. M. Kokhkharov, S.K. Nematov, R.A. Nusretov, V.O. Kuvondikov, A.A. Saparbaev. Opt. Spectrosc., **122**, 607 (2017). DOI: 10.1134/S0030400X1704021X
[40] F. Wu, H. Shi, Y. Gao, L. Cheng, T. Gu, T. Liu, Z. Chen, W. Fan. Sci. Reports., **14**, 1 (2024). DOI: 10.1038/s41598-024-80655-0
[41] L. Zhou, Y. Peng, N. Zhang, R. Du, R. Hübner, X. Wen, D. Li, Y. Hu, A. Eychmüller, L. Zhou, Y. Hu, R. Du, Y. Peng, X. Wen, D. Li, N. Zhang, A. Eychmüller, R. Hübner Helmholtz-Zentrum Dresden-Rossendorf, Adv. Opt. Mater., **9**, 2100352 (2021). DOI: 10.1002/adfm.202100352
[42] D. Kumar, Kavita, K. Singh, V. Verma, H. S. Bhatti. Appl. Nanosci., **5**, 881 (2015). DOI: 10.1007/s13204-014-0386-2
[43] L. Bardet, H. Roussel, S. Saroglia, M. Akbari, D. Muñoz-Rojas, C. Jiménez, A. Denneulin, D. Bellet. Nanoscale., **16**, 564 (2024). DOI: 10.1039/D3NR02663A

Translated by J.Savelyeva